JRMP Journal of Radiopharmaceuticals and Molecular Probes Vol. 3, No. 2, 2017
J Radiopharm Mol Probes 2017;3(2):72-79
ISSN 2384-1583(Print) / ISSN 2508-3848(Online)

ORIGINAL ARTICLE

https://doi.org/10.22643/JRMP.2017.3.2.72

Radio-Iodinated arbutin for tumor imaging

Phuong Tu Huynh[1], Yeong Su Ha[1], Woonghee Lee[1], Jeongsoo Yoo[1*]

[1] Department of Molecular Medicine, BK21 Plus KNU Biomedical Convergence Program, School of Medicine, Kyungpook National University, Daegu, Republic of Korea.

ABSTRACT

Arbutin is a hydroquinone derivative with a glucose moiety. As a tyrosinase inhibitor, it is widely used as a skin-whitening cosmetic agent for the treatment of cutaneous hyperpigmentary disorders, such as melasma and freckles. In the medical field, many studies have addressed the use of arbutin in various tumors, but the mechanism for tumor uptake of arbutin is still unclear. In this paper, we radiolabeled arbutin using radioiodine and studied its pharmacokinetics and tumor uptake via biodistribution experiments and single-photon emission computed tomography (SPECT) imaging. Radiolabeled ^{131}I-arbutin was stable for up to 24 h in PBS and serum. Biodistribution studies and SPECT imaging indicated high uptake of the compound in the bladder and kidneys shortly after injection. Twenty-four hours post-injection, significant deiodination was observed. Apart from high thyroid uptake, selective tumor uptake was clearly observed. The tumor-to-muscle and tumor-to-blood ratios were 26 and 9, respectively.

Key Word: arbutin, radioiodination, tumor imaging.

Introduction

Arbutin (4-hydroxyphenyl-β-D-glucopyranoside) is a glycosylated hydroquinone extracted from the fresh fruit of the California buckeye (1). It is known to inhibit tyrosinase, the rate-limiting enzyme for mammalian melanogenesis (2, 3, 4). Thus, arbutin is widely used as a skin-whitening cosmetic agent for the treatment of cutaneous hyperpigmentary disorders, such as melasma and freckles (2, 5). Since it is structurally related to hydroquinone, arbutin inhibits the activity of tyrosinase by interacting with the copper ions in its active site (6). It is used as an effective treatment for hyperpigmentary disorders and exhibits lower melanocyte cytotoxicity than hydroquinone itself. Arbutin inhibits melanogenesis by competitively and reversibly binding to tyrosinase, rather than influencing transcription of the tyrosinase gene (7). The compound not only inhibits tyrosinase but simultaneously causes maturation of melanosomes, plausibly as a result of its effects on 5, 6-dihydroxyindole-2-carboxylic acid (DHICA) polymerase activity and the silver protein in these organelles (8).

In the medical field, many studies have investigated the use of arbutin in various tumors, although the associated mechanisms are still poorly understood. For instance, it has been reported that arbutin acts as a potential anti-tumor agent in A375 human malignant melanoma

Received: December 08, 2017/ Revised: December 19, 2017/ Accepted: December 22, 2017

Correspnding Author : Jeongsoo Yoo, Department of Molecular Medicine, BK21 Plus KNU Biomedical Convergence Program, School of Medicine, Kyungpook National University, 680 Gukchaebosang-ro, Joon-gu, Daegu, 702-422, Korea
Tel: 82-53-420-4947, Fax: 82-53-426-4944, Email: yooj@knu.ac.kr.

cells (9). Li et al. determined the effects of arbutin on proliferation of the human bladder carcinoma cell line, TCCSUP, and reported that arbutin blocks TCCSUP cell proliferation through ERK inactivation and p21 expression upregulation (10). Furthermore, in human malignant melanoma cells, arbutin has been shown to cause VDAC1 overexpression and induce apoptosis (9, 11). Ye et al. studied some compounds, including arbutin, that bind to the pyruvate kinase isozyme PKM2, an important enzyme for glycogen metabolism whose expression is increased in most cancer cells (12, 13). Moreover, it is well known that compared with non-transformed tissue, cancerous tissues use large amounts of glucose and exhibit high rates of aerobic glycolysis (14); this phenomenon is known as the Warburg effect and is considered one of the hallmarks of cancer (14, 15). Arbutin, which is comprised of a glucose moiety conjugated to hydroquinone, can therefore be targeted to tumors.

Radioactive isotopes of iodine have proven to be very effective for labeling both large and small molecules (16), and radioiodination is one of the simplest methods for radiolabeling various biomolecules. Some common oxidizing agents used for this purpose include chloramine T, Iodobead, and Iodogen. Additionally, radioiodination enables radiolabeling at the ortho position of a phenol group. The aim of the present study was to radiolabel arbutin with radioiodine, and to assess the in vivo behavior and selective tumor uptake of the radiolabeled compound via biodistribution experiments and single-photon emission computed tomography (SPECT) imaging.

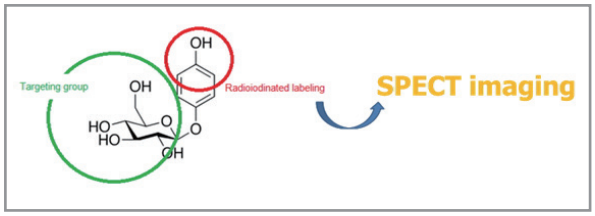

Figure 1. Chemical structure of arbutin

Materials and Methods

Materials

All chemicals were purchased from Sigma, including arbutin (≥ 98% purity), chloramine T trihydrate (ACS reagent, 98% purity), sodium metabisulfite (ACS reagent, ≥ 97.0% purity), and trifluoroacetic acid (TFA; reagentPlus®, 99% purity). Deionized distilled water (Milli-Q Gradient, Millipore) for the mobile phase was acidified with TFA (0.1%). Phosphate-buffered saline (PBS) was obtained from Hyclone. All other chemicals were of analytical grade.

Chromatographic conditions

Identification and purification of radiolabeled arbutin was achieved using a high-performance liquid chromatography (HPLC) system equipped with ultraviolet and radio detectors (Waters, Milford, MA, USA). Elution was performed under isocratic conditions with a mobile phase consisting of 100% water (0.1% TFA) vacuum-filtered through 0.45-μm nylon membranes (Germany) and carefully degassed before using. The flow-rate was 1 mL/min. Arbutin was detected at a wavelength of 220 nm. Two types of columns (250 × 4.6 mm, 5 μm, C18 GraceSmart and 50 × 4.6 mm, 5 μm, C5 Phenomenex) were used for optimization.

A radio thin-layer chromatography (radio TLC) scanner was used to monitor the radiolabeling yield of ^{131}I-arbutin after different reaction times. The stationary phase was C18 and the mobile phase was MeOH:10% NH_4OAc (1:1).

Radiochemistry

A 10 mg/mL stock solution of arbutin was prepared in MeOH, and a 100 μg/mL standard solution was prepared from the stock solution. Ten microliters of the arbutin stock solution (100 μg) was added to 100 μL deionized distilled water, mixed with $Na^{131}I$ (100 μCi), and shaken at 750 rpm for 1 min at room temperature. Next, chloramine T was added; various concentrations of chloramine T and various reaction times were tested for optimization. The reaction was terminated by the addition of sodium metabisulfite (100 μg in 10 μL) before purification of the product by HPLC.

Serum stability

For stability studies, approximately 100 μCi of the radiolabeled compound 131I-arbutin, purified by HPLC, was added to 500 μL PBS or 500 μL human serum. The resulting mixtures were incubated at 37 °C with shaking at 750 rpm. The radiolabeled compound was detected by radio TLC (C18, MeOH:10% NH4OAc) at various time points (0-24 h).

Biodistribution studies

All animal experiments were conducted in compliance with the Animal Care and Use Committee requirements of Kyungpook National University. CT26 murine colon cancer cells were cultured in RPMI 1640 containing 10% fetal bovine serum (FBS) and 1% penicillin/streptomycin at 37 °C in a 5% CO_2 atmosphere. Female BALB/c mice at 9 weeks of age were obtained from Hyochang Science (Daegu, Korea). The mice were injected subcutaneously in the right femoral region with 5×10^6 CT26 cells suspended in 100 μL RPMI 1640. When the tumors reached 9-10 mm in diameter (7–10 days after implantation), the mice were used for biodistribution studies. The mice were anesthetized with 1–2% isoflurane in 100% O_2 during injection, and then sacrificed 30 min or 24 h after injection. Tissues were then collected, and the radioactivity of the tissue samples was measured using a gamma counter (PerkinElmer, Waltham, MA, USA). Data were expressed as the percentage of the injected dose per gram of tissue (% ID/g).

CT26 tumor-bearing mice were injected with ^{123}I-arbutin (~20 μCi) via the tail vein. After the appropriate uptake time (0.5 or 24 h), anesthesia was

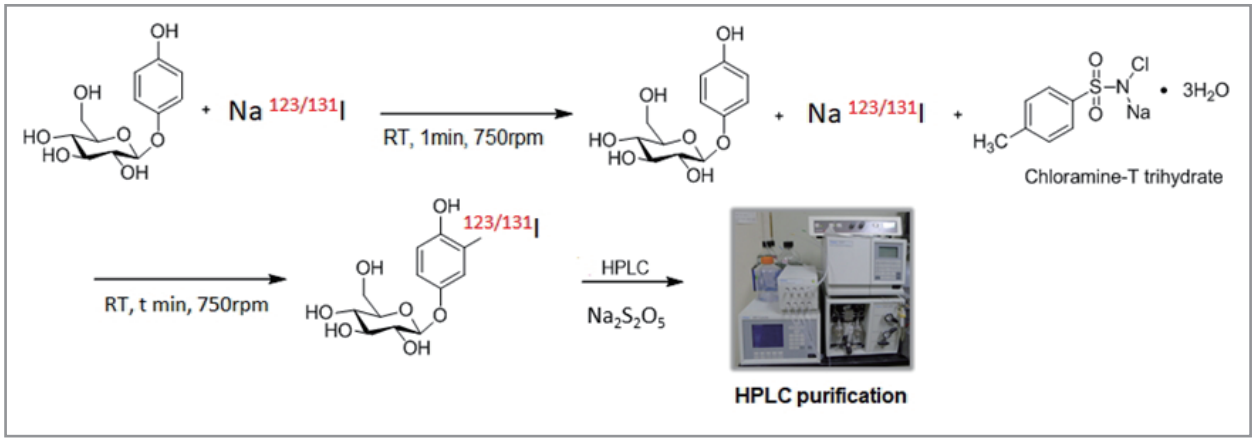

Scheme 1. Procedure for radiolabeling of arbutin.

induced with 2% isoflurane, and the mice were then positioned on the Inveon imaging system (Siemens Preclinical Solutions, Knoxville, TN, USA).

SPECT imaging

Data acquisition parameters for SPECT imaging were set to detect low-energy gamma photons with 25-s projections and 100 mm of bed travel. The multi-pinhole (whole-body mouse) collimator was used with a 35-mm radius of rotation. Data were reconstructed using a three-dimensional ordered subset expectation maximization (OSEM) algorithm (eight iterations and six subsets) onto an 88 × 88 × 312 matrix with isotropic 0.5-mm voxels.

Image analysis was performed by drawing regions of interest (ROIs) over the liver, spleen, heart, lungs, muscle, stomach, bladder, intestines, and kidneys. The mean voxel intensity associated with each ROI was recorded and used to compare the ROIs from all imaging time points. SPECT images were recorded 90 min post-injection.

Results and Discussion

1. Optimization of an HPLC/UV procedure for arbutin determination

In one study (17), arbutin was separated on an ODS Hypersil C18 column (125 mm × 4 mm, 5.0 μm) using a mobile phase of water:methanol:0.1 M hydrochloric acid (89:10:1, v/v/v) and a flow rate of 1.0 mL/min. Under these conditions, the retention time of arbutin was 5.7 min. In another study (18), arbutin was separated from hydroquinone using a Symmetry RP18 column (250 × 4.6 mm, 5 μm; Waters, Milford, MA, USA) together with gradient elution using a mobile phase of aqueous phosphoric acid (pH 3) and acetonitrile. The flow-rate was 1 mL/min, and the retention time of arbutin was 4.7 min. However, when we attempted HPLC purification of arbutin under the same conditions using a C18 GraceSmart column (250 × 4.6 mm, 5.0 μm), the arbutin peak was observed at 3.5 min, coinciding with the solvent peak (data not shown). Accordingly, we reoptimized the conditions for purification of arbutin by HPLC. Under the optimized conditions, HPLC/UV was performed under isocratic conditions using deionized distilled water (0.1% TFA) as the mobile phase and a flow rate of 1.0 mL/min. Arbutin is a small, hydrophilic molecule (molecular weight, 272.25 g/mol); therefore, when a C18 column (250 × 4.6 mm, 5 μm, C18 GraceSmart) was used, the compound did not interact with the column, even in the absence of any organic solvents, such as methanol or acetonitrile, and eluted in the dead volume (retention

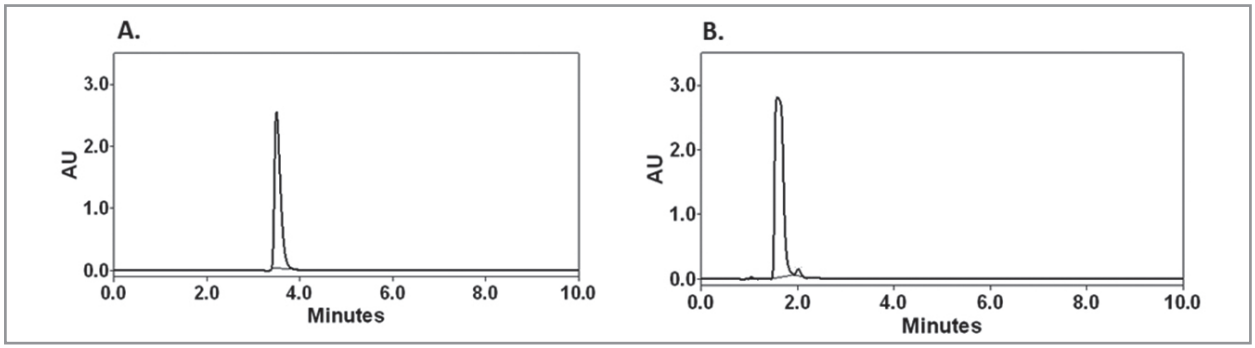

Figure 2. Optimization of HPLC/UV conditions for determination of arbutin using different columns. (A) 250 × 4.6 mm, 5 μm, C18 GraceSmart column. (B) 50 × 4.6 mm, 5 μm, C5 Phenomenex column.

time 3.5 min) (Fig. 2A). However, when a C5 column (50 × 4.6 mm, 5 μm, C5 Phenomenex) was used, arbutin eluted with a retention time of 1.6 min, which was later than the dead volume (retention time 1 min) (Fig. 2B). The purity of the compound (97.6%) was consistent with the purity stated by the manufacturer (Fig. 2B).

2. Optimization of the ^{131}I radiolabeling reaction using chloramine T

For labeling, ^{131}I solution (100 μCi) was mixed with 100 μg arbutin (10 μL) in 100 μL deionized distilled water. The mixture was incubated at room temperature with shaking at 750 rpm for 1 min, and then the reaction was initiated by the addition of 10 μL chloramine T at various concentrations (10 μg, 50 μg, or 100 μg in 10 μL water). After 15 min of incubation at room temperature with shaking at 750 rpm, the reaction was quenched by the addition of sodium metabisulfite (100 μg in 10 μL PBS). We optimized the radiolabeling reaction by using different concentrations of chloramine T (10 μg, 50 μg, or 100 μg in 10 μL water). When a high concentration of chloramine T (100 μg/10 μL) was used, two peaks were observed in the radio-HPLC chromatogram, with retention times of 8.3 min and 19.9 min. When the concentration of chloramine T was decreased, the magnitude of the second peak decreased and the magnitude of the first peak increased (Fig. 3). Based on the structures of mono-iodinated and di-iodinated arbutin as well as the principle of the radioiodination method, in which chloramine T is used as an oxidizing agent, we can assume that the first peak corresponds to the mono-iodinated compound, which was the main product when low concentrations of chloramine T

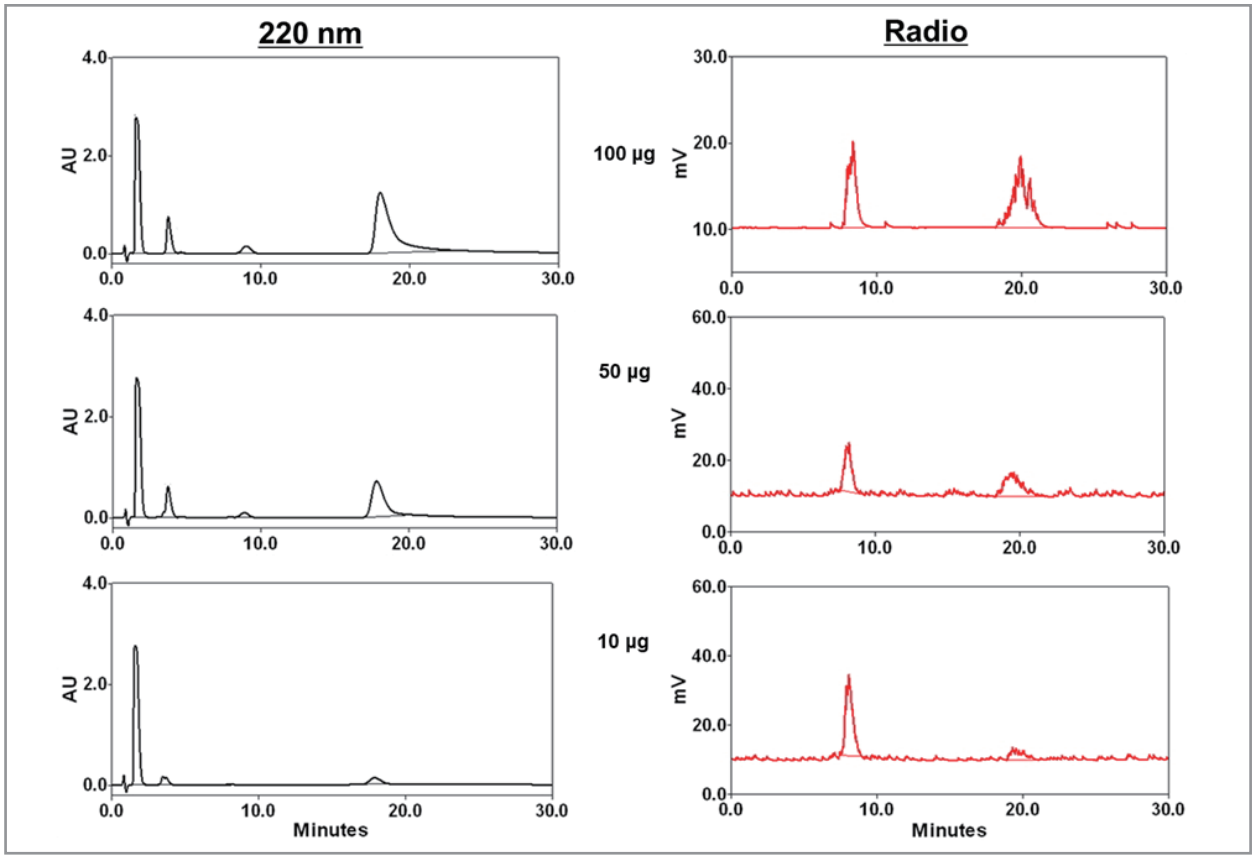

Figure 3. UV/radio-HPLC chromatograms of 131I-arbutin derivatives.

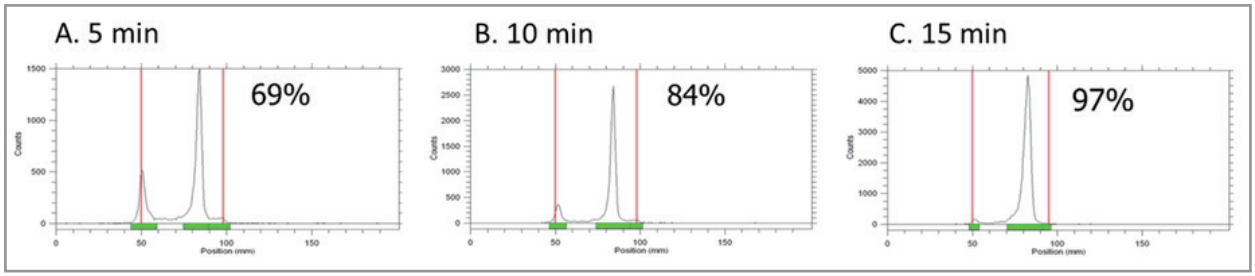

Figure 4. Radiolabeling yield of ^{131}I-arbutin after different reaction times. (A) 5 min, (B) 10 min, (C) 15 min.

were used, while the second peak corresponds to the di-iodinated compound. When high concentrations of the oxidizing agent are used, the compound to be labeled is exposed to harsh oxidizing conditions, which may affect its physicochemical properties. Therefore, we used the lowest concentration of chloramine T for radiolabeling purposes.

In addition to the concentration of the oxidizing agent, chloramine T, the reaction time could also have an effect on radiolabeling yield. Therefore, we measured the radiolabeling yield after reaction times of 5 min, 10 min, and 15 min using a radio TLC scanner. The results indicated that arbutin was quantitatively labeled after a reaction time of 15 min (radiolabeling yield 97%) (Fig. 4).

3. Stability of ^{131}I-arbutin in PBS and human serum

According to Dong et al. (19), who studied the immunological detection of arbutin, labeling of arbutin with ^{125}I can have a significant effect on its physicochemical properties because of the relatively low molecular mass of the compound. Therefore, we next assessed the stability of ^{131}I-arbutin in PBS and human serum. After successfully radiolabeling arbutin with ^{131}I by reaction of the compound with chloramine T (10 μg in 10 μL) at room temperature for 15 min, we tested the stability of the radiolabeled compound for further in vivo experiments. Firstly, radiolabeled arbutin was purified by HPLC and divided into two samples. Each sample, which had an activity of 100 μCi, was mixed with 500 μL PBS or human serum and incubated for various time periods (0–24 h) at 37 °C with shaking at 750 rpm. The results showed that radioiodinated arbutin is stable in PBS as well as in human serum (Fig. 5).

4. Biodistribution experiments in the CT26 tumor model

In vivo biodistribution studies were performed in 9-week-old female Balb/c mice (n = 2) at the 30-min and 24-h time points. At the earlier time point (30 min), most activity was observed in the kidneys (5.4%, data not shown), indicating that 123I-arbutin is rapidly cleared through renal excretion. At the later time point (24 h), the highest uptake was observed in the thyroid (1.2%), which was strongly indicative of significant deiodination of the radioiodinated compound. Apart from the thyroid, the highest activity was observed in the tumor, followed by the stomach, liver, kidneys, heart, and lungs. The tumor-to-muscle ratio was 26 and the tumor-to-blood ratio was 9 (Fig. 6). Even though deiodination occurred to a significant extent in vivo, 131I-arbutin showed selective tumor uptake, especially at the later time point.

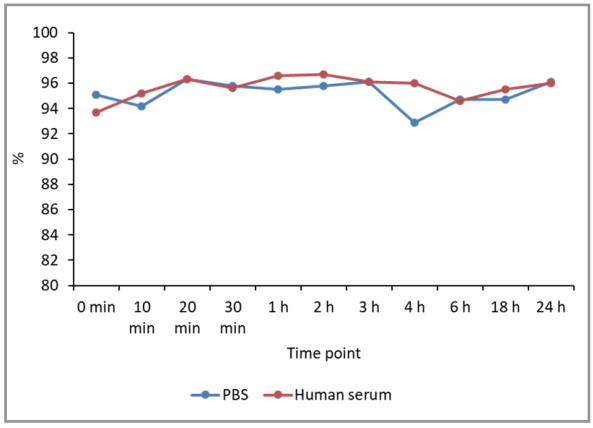

Figure 5. Stability of ^{131}I-arbutin in PBS and human serum.

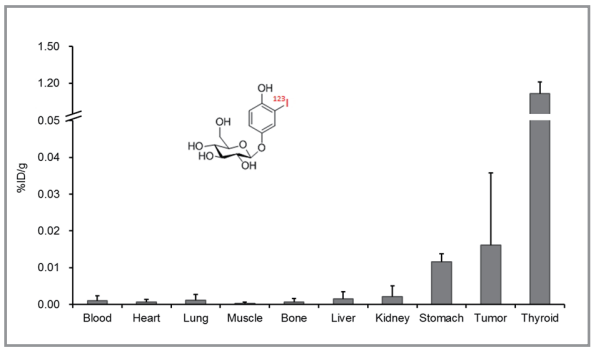

Figure 6. Biodistribution of ^{123}I-arbutin in the organs of female Balb/c mice 24 h after injection.

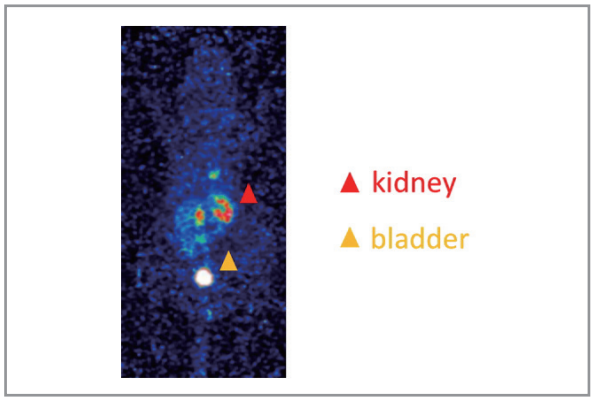

Figure 7. SPECT imaging of 123I-arbutin in CT26 tumor-bearing female Balb/c mice at 90 min post-injection.

5. SPECT imaging

SPECT imaging was performed 90 min after intravenous injection into the tail vein. SPECT imaging showed that most activity was found in the bladder and kidneys (Fig. 7), which was consistent with the results of the biodistribution experiments. This result confirmed that 131I-arbutin is rapidly cleared through renal excretion.

Conclusion

Radiolabeling of arbutin with 123/131I using chloramine T was completed within 15 min at room temperature. The radiolabeled 131I-arbutin was stable for up to 24 h in human serum. Biodistribution studies and SPECT imaging, which were performed in CT26 tumor model mice, showed high uptake of radioiodinated arbutin in the bladder and kidneys at early time points. After 24 h, the biodistribution data showed high thyroid uptake as a result of deiodination. However, except in the thyroid, high tumor-to-background ratios were obtained 24 h post-injection.

Acknowledgment

This work was supported by an R&D program through the National Research Foundation of Korea funded by the Ministry of Science, ICT & Future Planning (No. 2016R1A2B4011546, 2017M2C2A1014006 and 2017M2A2A6A02018506) and a grant of the Korea Health Technology R&D Project through the Korea Health Industry Development Institute (KHIDI) funded by the Ministry of Health & Welfare, Republic of Korea (HI17C0221).

References

1. Kubo I, Ying BP. Phenolic constituents of California buckeye fruit. *Phytochemistry* 1992;31:3793-3794.
2. Maeda K, Fukuda M. Arbutin: mechanism of its depigmenting action in human melanocyte culture. J Pharmacol Exp Ther

1996;276:765-769.
3. Sugimoto K, Nishimura T, Nomura K, Sugimoto K, Kurik T. Inhibitory effects of alpha-arbutin on melanin synthesis in cultured human melanoma cells and a three-dimensional human skin model, *Biol Pharm Bull* 2004;27:510-514.
4. Solano F, Briganti S, Picardo M, Ghanem G. Hypopigmenting agents: an updated review on biological, chemical and clinical aspects. *Pigment Cell Res* 2006;19:550-571.
5. Ertam I, Mutlu B, Unal I, Alper S, Kivcak B, Ozer O. Efficiency of ellagic acid and arbutin in melisma: a randomized, prospective, open-label study. *J Dermatol* 2008;35:570-574.
6. Lin JW, Chiang HM, Lin YC, Wen KC. Natural Products with Skin - Whitening Effects. *J Food Drug Anal* 2008;16:1-10.
7. Ebanks JP, Wickett RR, Boissy RE. Mechanisms regulating skin pigmentation: the rise and fall of complexion coloration. *Int J Mol Sci* 2009;10:4066-4087.
8. Chakraborty AK, Funasaka Y, Komoto M, Ichihashi M. Effect of arbutin on melanogenic proteins in human melanocytes. *Pigment Cell Res* 1998;11: 206-212.
9. Cheng SL, Liu RH, Sheu JN, Chen ST, Sinchaikul S, Tsay GJ. Toxicogenomics of A375 human malignant melanoma cells treated with arbutin. *J Biomed Sci* 2007;14:87-105.
10. Li H, Jeong YM, Kim SY, Kim MK, Kim DS. Arbutin inhibits TCCSUP human bladder cancer cell proliferation via up-regulation of p21. *Pharmazie* 2011;66:306-309.
11. Nawarak J, Huang-Liu R, Kao SH, Liao HH, Sinchaikul S, Chen ST, Cheng SL. Proteomics analysis of A375 human malignant melanoma cells in response to arbutin treatment. *Biochim Biophys Acta* 2009;1794:159-167.
12. Ye X, Sun Y, Xu Y, Chen Z, Lu S. Integrated in Silico-In Vitro Discovery of Lung Cancer-related Tumor Pyruvate Kinase M2 (PKM2) inhibitors. *Med Chem* 2016;12:613-620.
13. Warburg O, Wind F, Negelein E. THE METABOLISM OF TUMORS IN THE BODY. *J Gen Physiol*. 1927;8:519-530.
14. Hanahan D, Weinberg RA. Hallmarks of cancer: the next generation. *Cell.* 2011; 144:646-674.
15. Calvaresia EC, Hergenrother PJ. Glucose conjugation for the specific targeting and treatment of cancer. *Chem Sci* 2013;4: 2319-2333.
16. Seevers RH, Counsell RE. Radioiodination techniques for small organic molecules. *Chem Rev* 1982;82:575-590.
17. Thongchai W, Liawruangrath B, Liawruangrath S. High-performance liquid chromatographic determination of arbutin in skin-whitening creams and medicinal plant extracts. *J Cosmet Sci* 2007;58:35-44.
18. Gallo FR, Pagliuca G, Multari G, Panzini G, D'amore E, Altieri I. New High-performance Liquid Chromatography-DAD Method for Analytical Determination of Arbutin and Hydroquinone in Rat Plasma, *Indian J Pharm Sci* 2015;77:530-535.
19. Dong M, Li G, Li J, Zhou F, Gong Y, Zhang X, Zhao N. Immunological detection of arbutin, *Tsinghua Sci Technol* 1999; 4:1509-1514.